Available online at www.sciencedirect.com
SCIENCE DIRECT®
Solid State Communications 129 (2004) 721–725
solid state communications
www.elsevier.com/locate/ssc

Temperature dependence of electron magnetic resonance and magnetization in NiO nanorods

M.S. Seehra*, P. Dutta, H. Shim, A. Manivannan

Department of Physics, West Virginia University, Hodges Hall, Morgantown, WV 26506-6315, USA

Received 24 September 2003; received in revised form 9 December 2003; accepted 11 December 2003 by C. Lacroix

Abstract

For NiO nanorods of 5 nm diameter prepared by sol–gel technique, variations of the magnetization M with temperature T (5–370 K) and magnetic field H up to 55 kOe are reported. Also, temperature variations of the EMR (electron magnetic resonance) parameters (intensity I_0, linewidth ΔH and resonance field H_r) of an observed line due to uncompensated spins are followed for $T \leq 300$ K. The M vs. H and T variations yield a blocking $T_B \simeq 250$ K, above which the data fits modified Langevin function with magnetic moment $\mu_p \simeq 1240\ \mu_B$/particle. For the EMR line, I_0 decreases rapidly for $T < T_B$, and the line broadens and shifts to lower H with lowering T, following the lineshift $\delta H_r = (\Delta H)^n$ with $n \simeq 2.8$. This is close to the value of $n = 3$ expected for randomly oriented particles.

PACS: 75.50Tt; 75.20. − g; 75.50.Ee; 76.50. + g

Keywords: A. Nanostructures; A. Magnetically ordered materials; E. Electron magnetic resonance

The nature of magnetic ordering in bulk NiO (NaCl structure) has been known for over 40 years [1]. It is a type-2 antiferromagnet (AF) with the Néel temperature $T_N \simeq 523$ K such that the Ni^{2+} moments lying in the (111) planes are parallel, with the adjoining (111) planes stacked antiferromagnetically. Neutron scattering experiments [2] and temperature variations of the principal magnetic susceptibilities in single crystals of NiO [3] showed large spin reduction of $\Delta S = 0.19$ for the nominal $S = 1$ for Ni^{2+}. The nearest- and next-nearest-neighbor exchange constants, J_1 and J_2, respectively, have been determined to be: $J_1 = 34$ K and $J_2 = 202$ K [3]. Since T_N for NiO is above room temperature, it is a favorite component of spin-valve devices which require an antiferromagnet strongly coupled to a ferromagnet to produce exchange bias [4]. For this and reasons discussed below, it is of great interest to investigate how the magnetic properties of NiO are affected with reduction in size.

In recent years, a number of studies have been reported on the magnetic properties of nanoparticles (NP) of NiO [5–8]. Similar to other AF systems such as CuO [9], ferrihydrite and ferritin [10–12], NP of NiO are observed to become superparamagnet (SP) with decrease in particle size [5–8]. In such SP systems, the magnetization M above the blocking temperature T_B usually follows the modified Langevin behavior:

$$M = M_0\, \mathcal{L}(\mu_p H/k_B T) + \chi_a H \quad (1)$$

where μ_p is the magnetic moment/particle, and χ_a is the AF component of the susceptibility usually estimated from the high field region where the Langevin function $\mathcal{L}(x) = \coth x - (1/x)$ is nearly saturated. In AF nanoparticles, the source of M_0 is departure from complete AF compensation, generally valid for the NP surface spins.

Studies by Berkowitz et al. [6–8] have indicated that the M vs. H data in the NiO-NP system does not quite fit Eq. (1), although a large $\mu_p \simeq 2000\mu_B$ was inferred. Also, change in the nature of magnetic ordering may occur for smaller particles [6]. Recently, Rubinstein et al. [13] have reported on the temperature dependence of the electron magnetic

* Corresponding author. Tel.: +1-304-293-3422x1473; fax: +1-304-293-5736.
E-mail address: mseehra@wvu.edu (M.S. Seehra).

0038-1098/$ - see front matter © 2003 Elsevier Ltd. All rights reserved.
doi:10.1016/j.ssc.2003.12.019

resonance (EMR) spectra of 6 nm NiO particles. Similar to the observations reported in ferrihydrite NP [14], the resonance line was observed to shift to lower fields with decrease in temperature. However, the observed line shapes were very complex and distorted so that the linewidth ΔH and the resonance field H_r could not be measured accurately and hence their temperature variations could not be compared with the predictions for nanoparticle systems [15].

In this paper, we report on the temperature variation of ΔH and H_r in 5 nm nanorods of NiO, along with the temperature and magnetic fields variation of its magnetization M. It is observed that as the diameter D of the nanorods increases, the strength of the EMR signal decreases dramatically, mirroring the D dependence of M_0 determined from the fit to Eq. (1). Only for the 5 nm samples, the EMR lines at higher T are sufficiently well defined so that a quantitative check on the Nagata–Ishihara relation $\Delta H_r = (\Delta H)^n$ could be made (δH_r is the shift in the resonance field) [15]. Details of these results and their discussion are presented below.

The samples of NiO-NP were prepared using the procedures described by others [5–8]. This procedure consists of first synthesizing $Ni(OH)_2$ gel by reacting $Ni(NO_3)_2{\cdot}6H_2O$ with NaOH, followed by annealing $Ni(OH)_2$ at 523 K to produce the (5 ± 0.5) nm particles as determined from line-broadening (Scherrer relation) in X-ray diffraction. Annealing at higher temperatures of 573, 623, 673, 773 and 873 K produced particles of size 7, 8, 12, 16 and 20 nm, respectively. Transmission electron microscopy (TEM) of the 5 nm samples show these to be nanorods of various lengths with diameter $D \simeq 5$ nm and the EMR data is presented only for this sample for reason noted above. The EMR measurements were done at 9.28 GHz using a standard reflection-type cavity, a Varian magnet and an Oxford Instruments cryostat for variable temperature studies. The EMR measurements were done with decreasing temperatures, starting from room temperature to 4 K. For each temperature, the temperature is first stabilized followed by scanning the magnetic field from 100 to 10,100 Oe (for $H < 100$ Oe, the magnetic field in our electromagnet is somewhat unstable because of the residual field of the pole caps). Thus the EMR measurements simulate the field-cooled (FC) case. Measurements of the magnetization M vs. H and T were done using a commercial SQUID (superconducting quantum interference device) magnetometer.

The temperature variation of the magnetic susceptibility χ for the zero-field-cooled (ZFC) and field-cooled (FC) cases for the 5 nm sample are shown in Fig. 1, whereas Fig. 2 shows the plots of M vs. H at different T above the peak temperature $T_p \simeq 200$ K. The magnitudes of χ in Fig. 1 are nearly two orders of magnitude larger than that for bulk NiO [3], signifying dominant contribution from nanoparticle effects. Fitting of the M vs. H data of Fig. 2 to Eq. (1) yields the plot of $(M - \chi_a H)/M_0$ against H/T shown in Fig. 3, with

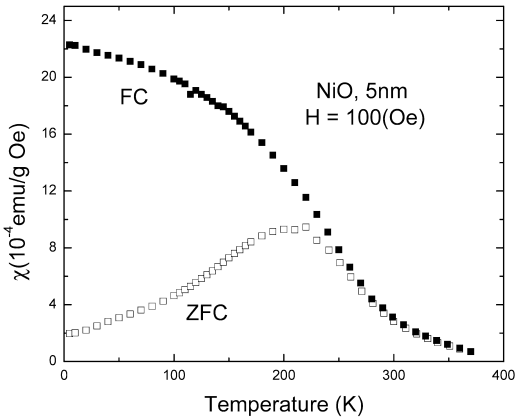

Fig. 1. Temperature dependence of the magnetic susceptibility χ for FC (field-cooled) and ZFC (zero-field-cooled) cases.

$\mu_p = 1240\mu_B$, as the magnetic moment per particle. The source of μ_p and M_0 is the uncompensated spins because in bulk NiO, $\mu_p = 0$ due to complete compensation of antiferromagnetic ordering. In the inset of Fig. 3, we show the temperature variations of M_0 and χ_a determined from these fits. The collapse of the data onto a single curve in Fig. 3 provides evidence for superparamagnetism and temperature variations of M_0 and χ_a are similar to those reported in other AF-NP systems [9–12]. By extrapolating M_0 to zero in the inset of Fig. 3, $T_N \simeq 400$ K is determined for the 5 nm NiO nanorods.

The behavior of the EMR lines at different T is depicted in Fig. 4, where it is evident that on lowering T, line broadens and shifts to lower fields. The lines are very broad and Lorentzian-type, resulting in significant zero-field absorption even at room temperature. The peak-to-peak linewidths ΔH in the absorption derivative of Fig. 4 were measured as well as the resonance field H_r defined by the center of the peak-to-peak separation since the baseline is difficult to ascertain.

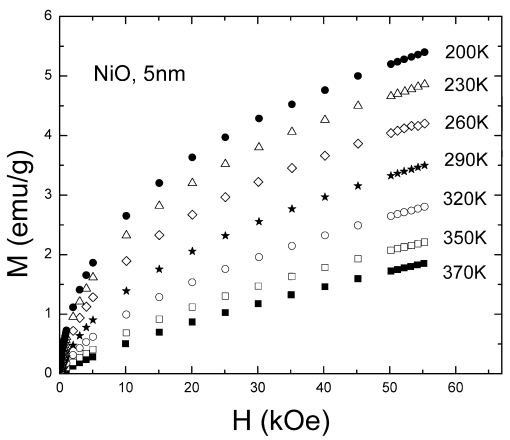

Fig. 2. Isothermal plots of the magnetization M against applied field H at temperatures shown.

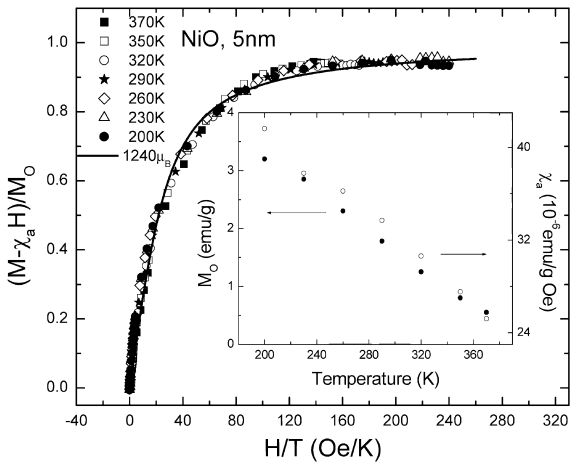

Fig. 3. Fitting of the M vs. H data to Eq. (1) yielding the plot of $(M - \chi_a H)/M_0$ vs. H/T. The solid line is the Langevin variation with $\mu_p = 1240\mu_B$. In the inset, temperature variations of M_0 and χ_a are shown.

The temperature variations of ΔH and H_r are shown in Fig. 5. Whereas, ΔH continues its monotonic increase with decrease in temperature, the resonance field H_r begins its rapid decrease only below 250 K. Comparing this with the χ vs. T variation of Fig. 1, it is evident that the bifurcation between the FC and ZFC, suggestive of blocking, also begins to occur below about 250 K. A more convincing evidence of spin-freezing below 250 K is evident in Fig. 6 where we have plotted peak-to-peak height h and the computed intensity $I_0 = (\Delta H)^2 h$ against temperature. A rapid decrease in both h and I_0 below 250 K is indicative of loss of paramagnetic spins to blocking or freezing. A second weaker anomaly is observed in all the EMR parameters below $T_p \simeq 200\,K$ of Fig. 1. It should be noted that to calculate EMR intensity, ideally one should measure the area under the curve by double integration of the derivative signals of Fig. 4. In the present case, because of large zero-field absorption, such a procedure would be incorrect. However, as long as there is no change in the lineshape, $I_0 = (\Delta H)^2 h$ should provide an accurate estimate of the changes of I_0 vs. T [16].

A phenomenological model for changes in H_r and ΔH in magnetic NP systems with decreases in temperature was advanced by Nagata and Ishihara [15], and it has been tested in Mn-Zn ferrite particles [15] and ferrihydrite NP [14]. The model assumes NP of ellipsoidal shape and distinguishes between the aligned case where the major axis of the ellipsoid are along the applied field and the case with the major axes oriented randomly with respect to field. The demagnetization field, which depends on the shape anisotropy and magnetization, then produces changes in H_r and ΔH. The model predicts $\delta H_r \simeq (\Delta H)^n$, where $n = 2$ for partially oriented and $n = 3$ for randomly oriented particles. In the data of Fig. 5, H_r increases only weakly with T from 250 to 300 K. Using the g-value of 2.23 for NiO [3], $H_r = 2970\,Oe$ for paramagnetic resonance, a magnitude

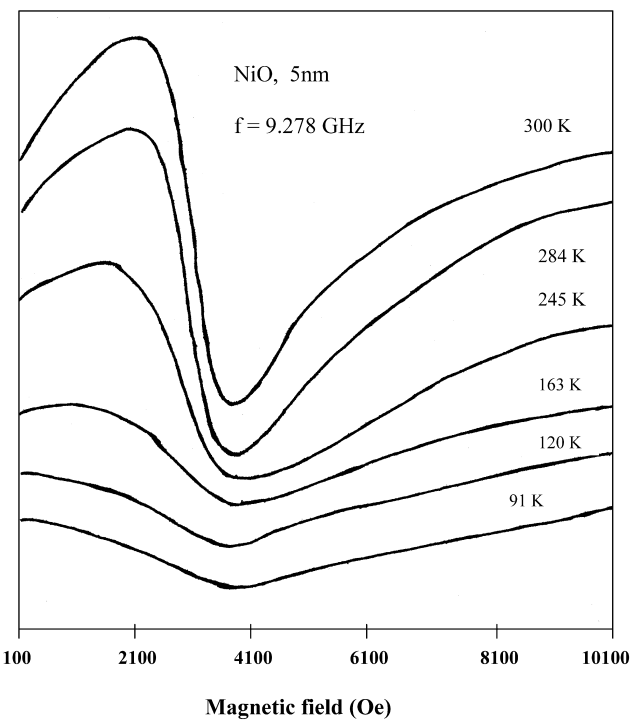

Fig. 4. Plots of the EMR derivative line for several temperatures.

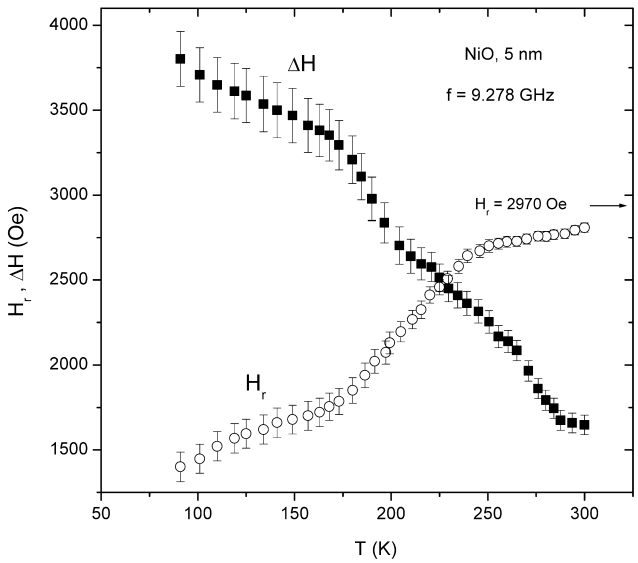

Fig. 5. Temperature variations of the linewidth ΔH and resonance field H_r. Arrow indicates the position of H_r for $g = 2.23$.

close to that measured at 300 K but it will be reached only at $T > 300\ K$. Therefore we have used $\delta H_r = 2970 - H_r(T)$ to make the log–log plot of Fig. 7. The slope yield $n \simeq 2.8$, close to the magnitude expected for randomly oriented particles [15].

In summary, results presented here on the temperature variation of magnetization and the EMR spectra of 5 nm NiO nanorods have established superparamagnetism with $\mu_p \simeq 1240\mu_B$/particle. Furthermore, blocking with decreasing T is accompanied by rapid decrease in the intensity of the EMR line, with its shift to lower field and broadening. The lineshifts and broadening are consistent with the theoretical predictions for randomly oriented particles. The rapid decrease in the EMR signal for larger NiO-NP suggests that the observed EMR signal is associated with the uncompensated spins. A detailed study on the morphology of the NiO particles

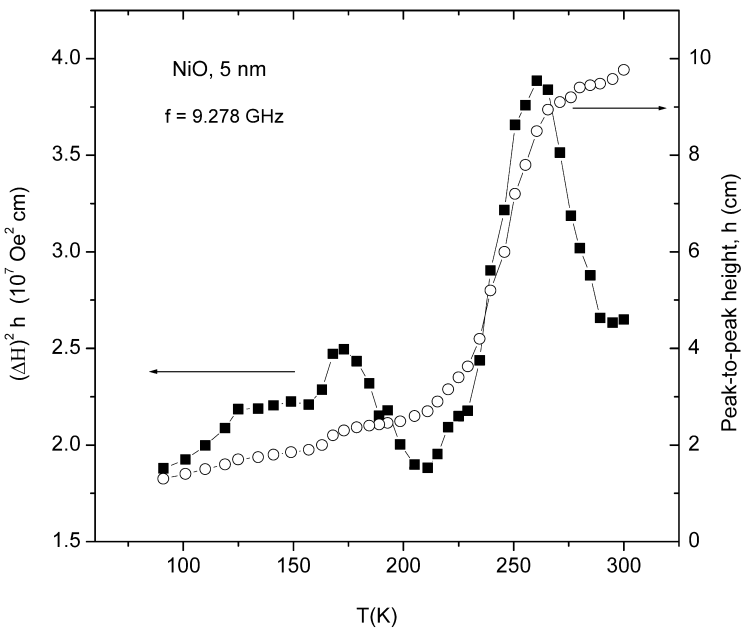

Fig. 6. Temperature variations of the intensity $I_0 = (\Delta H)^2 h$ and peak-to-peak height, h of the EMR signal.

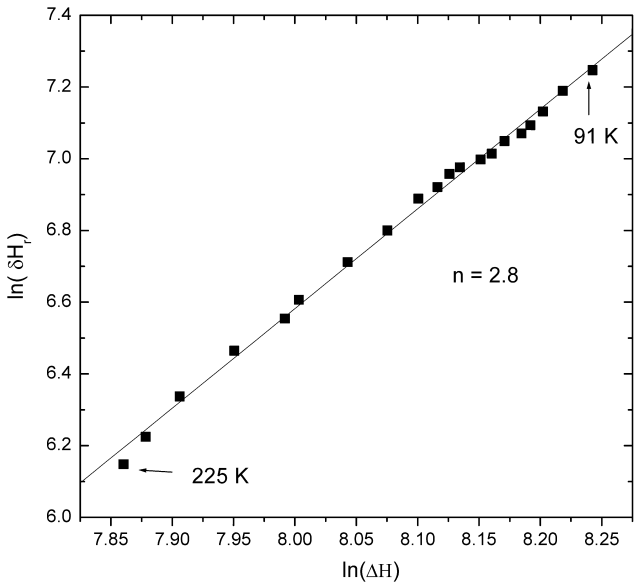

Fig. 7. ln–ln plot of $\delta H_r = 2970 - H_r$ against ΔH. The line through the points is a least-squares fit with slope = 2.8.

as determined by TEM and on the particle size dependence of the magnetic and structural properties of the NiO-NP system will be reported in the near future [17].

Acknowledgements

This work was supported by research grants from the US Department of Energy and the US Air Force Office of Scientific Research.

References

[1] W.L. Roth, Phys. Rev. 110 (1958) 1333. W.L. Roth, Phys. Rev. 111 (1958) 772. W.L. Roth, J. Appl. Phys. 31 (1960) 2000.
[2] H.A. Alperin, J. Phys. Soc. Jpn. Suppl. 17-B3 (1962) 12.
[3] G. Srinivasan, M.S. Seehra, Phys. Rev. B 29 (1984) 6295.
[4] A.E. Berkowitz, K. Takano, J. Magn. Magn. Mater. 200 (1999) 552 and references therein.
[5] J.T. Richardson, D.L. Yiagas, B. Turk, K. Forster, M.V. Twigg, J. Appl. Phys. 70 (1991) 6977.
[6] R.H. Kodama, A.E. Berkowitz, Phys. Rev. B 59 (1999) 6321.
[7] R.H. Kodama, S.A. Makhlouf, A.E. Berkowitz, Phys. Rev. Lett. 79 (1997) 1393.
[8] S.A. Makhlouf, F.T. Parker, F.E. Spada, A.E. Berkowitz, J. Appl. Phys. 81 (1997) 5561.
[9] A. Punnoose, H. Magnone, M.S. Seehra, J. Bonevich, Phys. Rev. B 64 (2001) 174420.
[10] M.S. Seehra, A. Punnoose, Phys. Rev. B 64 (2001) 132411.
[11] M.S. Seehra, V.S. Babu, A. Manivannan, J.W. Lynn, Phys. Rev. B 61 (2000) 3513.
[12] S.A. Makhlouf, F.T. Parker, A.E. Berkowitz, Phys. Rev. B 55 (1997) R14717.
[13] M. Rubinstein, R.H. Kodama, S.A. Makhlouf, J. Magn. Magn. Mater. 234 (2001) 289.
[14] M.S. Seehra, A. Punnoose, P. Roy, A. Manivannan, IEEE Trans. Magn. 37 (2001) 2007.
[15] K. Nagata, A. Ishihara, J. Magn. Magn. Mater. 104–107 (1992) 1571.
[16] C.P. Poole Jr., Electron Spin Resonance, 2nd ed., Dover, New York, 1983, p. 483.
[17] H. Shim, A. Manivannan, M. S. Seehra, J. Bonevich. In preparation.